Compact Elliptic-Function Low-Pass Filters Using Microstrip Stepped-Impedance Hairpin Resonators

Lung-Hwa Hsieh, *Student Member, IEEE*, and Kai Chang, *Fellow, IEEE*

***Abstract*—A compact elliptic-function low-pass filter using microstrip stepped-impendance hairpin resonators and their equivalent-circuit models are developed. The prototype filters are synthesized from the equivalent-circuit model using available element-value tables. To optimize the performance of the filters, electromagnetic simulation is used to tune the dimensions of the prototype filters. The filter using multiple cascaded hairpin resonators provides a very sharp cutoff frequency response with low insertion loss. Furthermore, to increase the rejection-band bandwidth, additional attenuation poles are added in the filter. The filters are evaluated by experiment and simulation with good agreement. This simple equivalent-circuit model provides a useful method to design and understand this type of filters and other relative circuits.**

***Index Terms*—Elliptic-function filter, low-pass filter, stepped-impendance hairpin resonator.**

I. Introduction

COMPACT SIZE and high-performance microwave filters are highly demanded in many communication systems. Due to the advantages of small size and easy fabrication, the microstrip hairpin has been drawing much attention. From the conventional half-wavelength hairpin resonator to the latest stepped-impendance hairpin resonator, a size reduction of the resonator has been dramatically achieved [1]–[6]. Conventionally, the behavior of the stepped-impendance hairpin resonator has been described by using even- and odd-mode and network models [2], [4]. However, they only showed limited expressions in terms of the $ABCD$ matrix, which do not provide a useful circuit design implementation such as equivalent lumped-element circuits.

Small-size low-pass filters are frequently required in many communication systems to suppress harmonics and spurious signals. The conventional stepped-impedance and Kuroda-identity-stubs low-pass filters only provide Butterworth and Chebyshev characteristics with a gradual cutoff frequency response [7]. In order to have a sharp cutoff frequency response, these filters require more sections. Unfortunately, increasing the number of sections also increases the size of the filter and insertion loss. Recently, the low-pass filter using photonic-bandgap and defect ground structures [8], [9] illustrated a similar performance as those of the conventional ones. A compact semilumped low-pass filter was also proposed [10]. However, using lumped elements increase the fabrication difficulties.

Manuscript received October 16, 2001.
The authors are with the Department of Electrical Engineering, Texas A&M University, College Station, Texas 77843-3128 USA (e-mail: welber@ee.tamu.edu; chang@ee.tamu.edu).
Digital Object Identifier 10.1109/TMTT.2002.806901

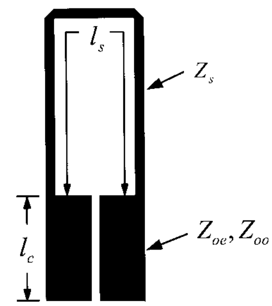

Fig. 1. Stepped-impendance hairpin resonator.

The microstrip elliptic-function low-pass filters show the advantages of high performance, low cost, and easy fabrication [11], [12]. In [12], the elliptic-function low-pass filters using elementary rectangular structures provide a wide-band passband with a sharp cutoff frequency response, but a narrow stopband.

In this paper, an equivalent-circuit model for the stepped-impendance hairpin resonator is described. A compact elliptic-function low-pass filter using the stepped-impendance hairpin resonator is also demonstrated. The dimensions of the prototype low-pass filters are synthesized from the equivalent-circuit model with the published element-value tables. The exact dimensions of the filter are optimized by electromagnetic (EM) simulation. The filter using multiple cascaded stepped-impendance hairpin resonators shows a very sharp cutoff frequency response with a low insertion loss. Furthermore, additional attenuation poles are added to suppress the second harmonic and achieve a broad stopband bandwidth. The measured results agree well with simulated results.

II. Equivalent-Circuit Model for the Step-Impedance Hairpin

Fig. 1 shows the basic layout of the stepped-impendance hairpin resonator. The stepped-impendance hairpin resonator consists of the single transmission line l_s and coupled lines with a length of l_c. Z_s is the characteristic impedance of the single transmission line l_s. Z_{oe} and Z_{oo} are the even- and odd-mode impedance of the symmetric capacitance-load parallel coupled lines with a length of l_c. By selecting $Z_s > \sqrt{Z_{oe} Z_{oo}}$, the size of the stepped-impendance hairpin resonator is smaller than that of the conventional hairpin resonator [13]. Also, the effect of the loading capacitance shifts the spurious resonant frequencies of the resonator from integer multiples of the fundamental resonant frequency, thereby reducing interferences from high-order harmonics.

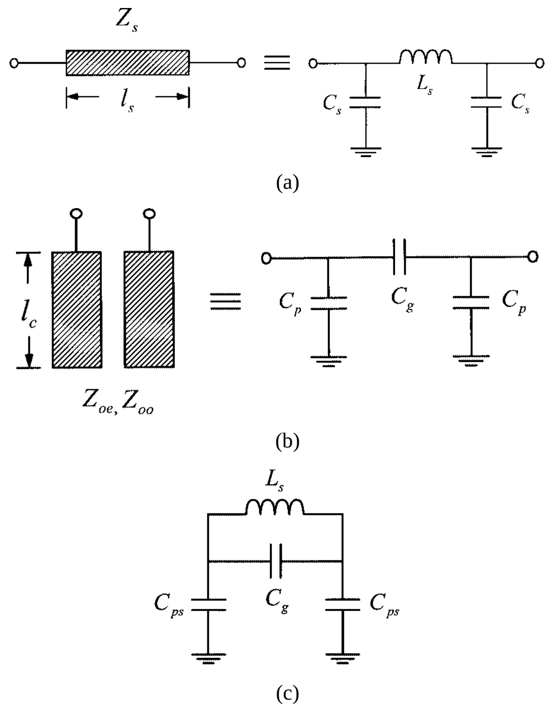

Fig. 2. Equivalent circuit of: (a) single transmission line, (b) symmetric coupled lines, and (c) stepped-impendance hairpin resonator.

The single transmission line is modeled as an equivalent *L*-*C* π-network, as shown in Fig. 2(a). For the lossless single transmission line with a length of l_s, the $ABCD$ matrix is given by

$$\begin{bmatrix} A & B \\ C & D \end{bmatrix} = \begin{bmatrix} \cos(\beta_s l_s) & jZ_s \sin(\beta_s l_s) \\ jY_s \sin(\beta_s l_s) & \cos(\beta_s l_s) \end{bmatrix} \tag{1}$$

where β_s and $Y_s = 1/Z_s$ are the phase constant and characteristic admittance of the single transmission line, respectively. The $ABCD$ matrix of the equivalent *L*-*C* π-network is

$$\begin{bmatrix} A & B \\ C & D \end{bmatrix} = \begin{bmatrix} 1 + Z_L Y_c & Z_L \\ Y_c(2 + Z_L Y_c) & 1 + Z_L Y_c \end{bmatrix} \tag{2}$$

where $Z_L = j\omega L_s, Y_c = j\omega C_s, \omega$ is the angular frequency, and L_s and C_s are the equivalent inductance and capacitance of the single transmission line. Comparing (1) and (2), the equivalent L_s and C_s can be obtained as

$$L_s = \frac{Z_s \sin(\beta_s l_s)}{\omega} \quad \text{(H)} \tag{3a}$$

and

$$C_s = \frac{1 - \cos(\beta_s l_s)}{\omega Z_s \sin(\beta_s l_s)} \quad \text{(F)}. \tag{3b}$$

Moreover, as seen in Fig. 2(b), the symmetric parallel coupled lines are modeled as an equivalent capacitive π-network. The $ABCD$ matrix of the lossless parallel coupled lines is expressed as [2]

$$\begin{bmatrix} A & B \\ C & D \end{bmatrix} = \begin{bmatrix} \dfrac{Z_{oe} + Z_{oo}}{Z_{oe} - Z_{oo}} & \dfrac{-j2Z_{oe}Z_{oo}\cot(\beta_c l_c)}{Z_{oe} - Z_{oo}} \\ \dfrac{j2}{(Z_{oe} - Z_{oo})\cot(\beta_c lc)} & \dfrac{Z_{oe} + Z_{oo}}{Z_{oe} - Z_{oo}} \end{bmatrix} \tag{4}$$

where β_c is the phase constant of the coupled lines. Also, the $ABCD$ matrix of the equivalent capacitive π-network is

$$\begin{bmatrix} A & B \\ C & D \end{bmatrix} = \begin{bmatrix} 1 + Z_g Y_p & Z_g \\ Y_p(2 + Z_g Y_p) & 1 + Z_g Y_p \end{bmatrix} \tag{5}$$

where $Z_g = 1/j\omega C_g$ and $Y_p = j\omega C_p$. In comparison with (4) and (5), the equivalent capacitances of the π-network are found as

$$C_g = \frac{Z_{oe} - Z_{oo}}{2\omega Z_{oe} Z_{oo} \cot(\beta_c l_c)} \quad \text{(F)} \tag{6a}$$

and

$$C_p = \frac{1}{\omega Z_{oe} \cot(\beta_c l_c)} \quad \text{(F)}. \tag{6b}$$

Furthermore, combining the equivalent circuits of the single transmission line and coupled lines, shown in Fig. 2(a) and (b), the equivalent circuit of the stepped-impendance hairpin resonator in terms of lumped elements L and C is shown in Fig. 2(c), where $C_{ps} = C_p + C_s + C_\Delta$ is the sum of the capacitances of the single transmission line, coupled lines, and the junction discontinuity (C_Δ) between the single transmission line and coupled lines [14].

The physical dimensions of the filter can be synthesized by using the available *L*-*C* tables and (3) and (6). The widths of the single transmission line and coupled lines of the filter can be obtained from selecting the impedances that satisfy the condition $Z_s > \sqrt{Z_{oe} Z_{oo}}$. The lengths of the single transmission line and coupled lines of the filter transformed from (3a) and (6b) are

$$l_s = \frac{\sin^{-1}(\omega_c L_{st}/Z_s)}{\beta_s} \tag{7a}$$

and

$$l_c = \frac{\tan^{-1}\left[\omega_c Z_{oe}(C_{pst} - C_s - C_\Delta)\right]}{\beta_c} \tag{7b}$$

where ω_c is the 3-dB cutoff angular frequency, and L_{st} and C_{pst} are the inductance and capacitance chosen from the available *L*-*C* tables. C_s and C_g can be calculated from (7a), (3b), (7b), and (6a), respectively.

III. Compact Elliptic-Function Low-Pass Filters

A. Low-Pass Filter Using One Stepped-Impedance Hairpin Resonator

Fig. 3 shows the geometry and equivalent circuit of the elliptic-function low-pass filter using one stepped-impendance hairpin resonator with feed lines l_f. As seen from the equivalent circuit in Fig. 3(b), L_s is the equivalent inductance of the single transmission line of the filter. C_g is the equivalent capacitance of the coupled lines and C_{ps} is sum of the capacitances of the transmission line l_1 and the coupled lines. Using the available elliptic-function element-value tables [15] with impedance and frequency scaling, the dimensions of the prototype low-pass filter can be approximately synthesized by (3a) and (3b), (6a) and (6b), and (7a) and (7b). The exact dimensions are adjusted to optimize the performance of the filter using EM simulation

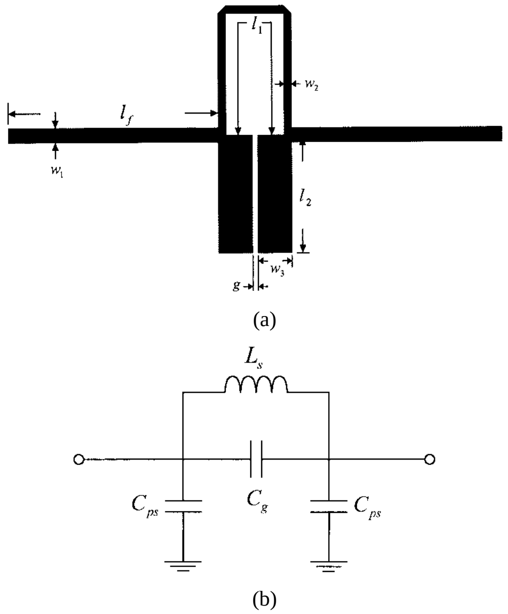

Fig. 3. Low-pass filter using one hairpin resonator. (a) Layout. (b) Equivalent circuit.

TABLE I
L-C VALUES OF THE FILTER USING ONE HAIRPIN RESONATOR

	C_{ps}	C_g	L_s
Available L-C tables	1.52 pF	0.13 pF	4.2 nH
Approximated L-C values	1.52 pF	0.22 pF	4.2 nH
Optimized L-C values	2.23 pF	0.34 pF	4.87 nH

software IE3D[1] to account for the loss and discontinuity effects not included in the lumped-element model of Fig. 3(b). The low-pass filter is designed for a 3-dB cutoff frequency of 2 GHz and fabricated on a 25-mil-thick RT/Duroid 6010.2 substrate with relative dielectric constant $\epsilon_r = 10.2$.

Table I shows the equivalent *L-C* values from the available *L-C* tables, approximated *L-C* values, and optimized *L-C* values, respectively. Observing the available *L-C* tables, the filter using one microstrip hairpin resonator is difficult to synthesize. An approximate synthesis is introduced by using some inductances and capacitances chosen from the available *L-C* tables and (3), (6), (7a), and (7b). For instance, using the inductance and capacitance L_s and C_{ps} in the available *L-C* tables, the lengths of the single and coupled lines can be found from (7a), (7b), and (3b), respectively. Also, the capacitance C_g can be obtained from (6a). Fig. 4 shows the simulated frequency responses of the filter using *L-C* values in Table I. The simulated frequency response of the filter with the available *L-C* tables is obtained using the Agilent ADS circuit simulator. The simulated frequency responses of the filter with the approximated and optimized *L-C* values are obtained using the IE3D EM simulator. Observing the simulated results in Fig. 4, the equal ripple response of the microstrip filter at the stopband is affected by the harmonics of the filter. The optimized filter with larger *L-C* values has a closer 3-dB cutoff frequency at 2 GHz and a better

[1]IE3D, ver. 8.0, Zeland Software Inc., Fremont, CA, Jan. 2001.

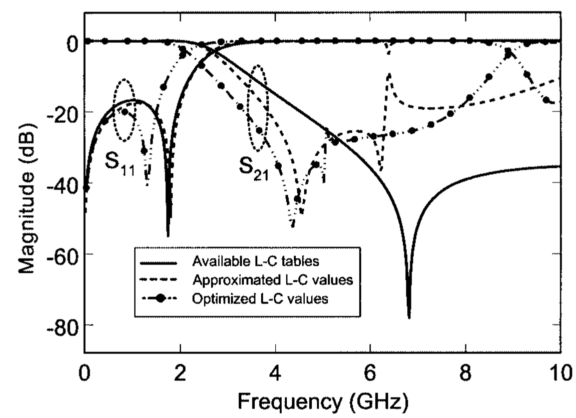

Fig. 4. Simulated frequency responses of the filter using one hairpin resonator.

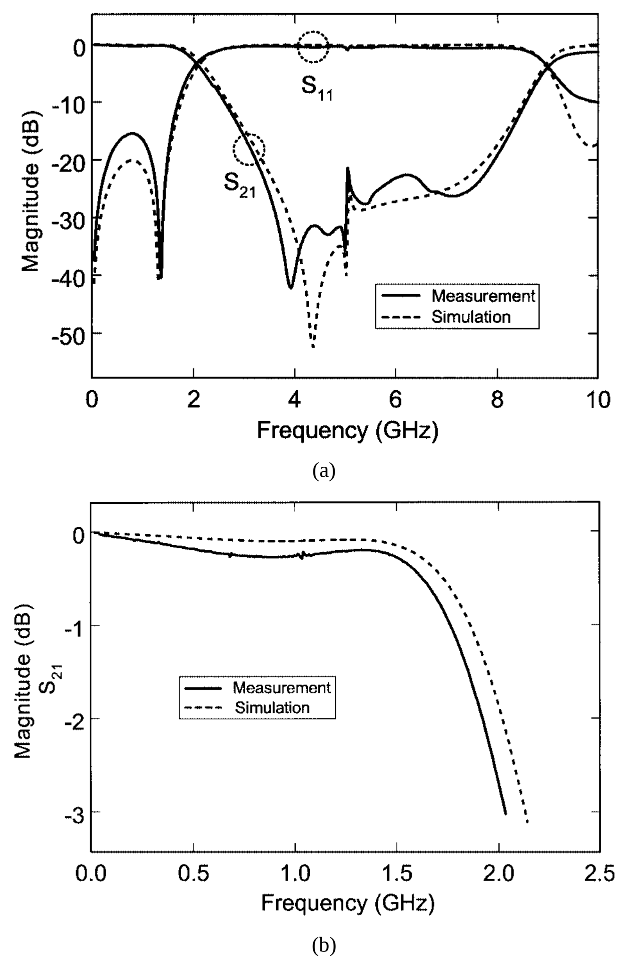

Fig. 5. Measured and simulated: (a) frequency response and (b) S_{21} within the 3-dB bandwidth for the filter using one hairpin resonator.

return loss. The optimized dimensions of the filter are $l_f = 8\,\text{mm}$, $l_1 = 11.92\,\text{mm}$, $l_2 = 4.5\,\text{mm}$, $w_1 = 0.56\,\text{mm}$, $w_2 = 0.3\,\text{mm}$, $w_3 = 1.31\,\text{mm}$, and $g = 0.2\,\text{mm}$. Fig. 5 shows the measured and simulated results of the filter with the optimized dimensions. Inspecting the measured results, the elliptic low-pass filter has a 3-dB passband from dc to 2.03 GHz. The insertion loss is less than 0.3 dB, and the return loss is better than 15 dB from dc to 1.57 GHz. The rejection is greater than 20 dB within 3.23–7.93 GHz. The ripple is ± 0.14 dB, as shown in Fig. 5(b).

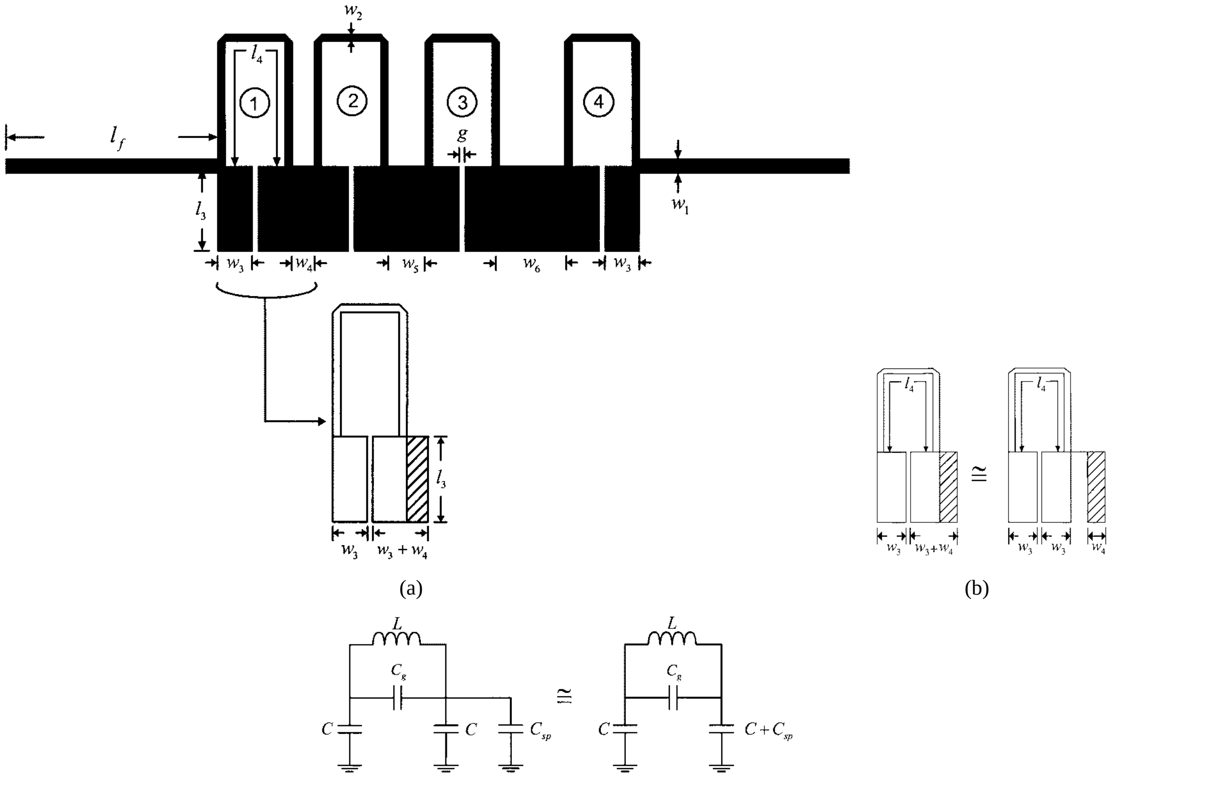

Fig. 6. Low-pass filter using cascaded hairpin resonators. (a) Layout. (b) Asymmetric coupled lines. (c) Equivalent circuit of the asymmetric coupled lines.

B. Low-Pass Filter Using Multiple Cascaded Stepped-Impedance Hairpin Resonators

Fig. 6(a) shows the low-pass filter using four multiple cascaded stepped-impendance hairpin resonators. Inspecting this structure, two resonators are linked by an adjacent transmission line with a width of w_4, w_5, or w_6. Due to the adjacent transmission line, the coupled lines become an asymmetrical coupling structure, as shown on the left-hand side of Fig. 6(b). The asymmetrical coupled lines can be roughly treated as a symmetric coupled lines with a separate parallel single transmission line, as shown on the right-hand side of Fig. 6(b) [16]. Therefore, as seen in Fig. 6(c), the equivalent circuit of the asymmetric coupled lines can be approximately represented by that of the symmetric coupled lines in Fig. 2(b) and a equivalent capacitance C_{sp} of a single transmission line in shunt. The equivalent capacitance C_{sp} is given by

$$C_{sp} = \epsilon_o \epsilon_r w/h \quad \text{(F/unit length)} \tag{8}$$

where w is the width of the adjacent transmission line and h is the substrate thickness. The equivalent circuit of the low-pass filter is illustrated in Fig. 7.

Table II shows the available *L-C* tables, approximated *L-C* values, and optimized *L-C* values of the filter using four cascaded hairpin resonators. Also, observing the available *L-C* tables, the inductances and capacitances between resonators show a high variation, of which is difficult to synthesize a low-pass filter using cascaded microstrip hairpin resonators. For example, by using the inductances and capacitances L_2, L_4, L_6, L_8, C_1, C_3, C_5, C_7, and C_9 in the available tables and (7a)–(8), the capacitances C_4 and C_6 calculated from (6a) are very small. In this case, the 3-dB cutoff frequency of the filter is larger than that of the filter using the available *L-C* tables. Moreover, if the filter is synthesized by using the inductances and capacitances L_2, L_4, L_6, L_8 C_2, C_4, C_6, and C_8 in the available tables and (3b), (7a), (8), and (9), then the capacitances C_3, C_5, and C_7 will become large, where (9), transformed from (6a) for the synthesized length of the coupled lines, is given by

$$l_c = \frac{\tan^{-1}\left[2\omega_c C_{gt} Z_{oe} Z_{oo}/(Z_{oe} Z_{oo})\right]}{\beta_c} \tag{9}$$

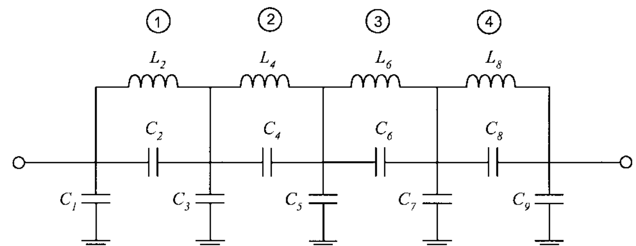

Fig. 7. Equivalent circuit of the low-pass filter using cascaded hairpin resonators.

TABLE II
L-C VALUES OF THE FILTER USING FOUR HAIRPIN RESONATORS

	C_1	C_2	L_2	C_3	C_4	L_4	C_5	C_6	L_6	C_7	C_8	L_8	C_9
Available L-C tables	1.98 pF	0.2 pF	5.07 nH	2.65 pF	1.21 pF	3.45 nH	1.95 pF	1.65 pF	2.9 nH	2.17 pF	0.74 pF	3.84 nH	1.56 pF
Approximated L-C values	1.98 pF	0.24 pF	5.07 nH	4.83 pF	0.61 pF	3.45 nH	4.97 pF	0.44 pF	2.9 nH	4.49 pF	0.45 pF	3.84 nH	2.16 pF
Optimized L-C values	1.79 pF	0.23 pF	4.89 nH	3.93 pF	0.23 pF	4.89 nH	4.48 pF	0.23 pF	4.89 nH	3.93 pF	0.23 pF	4.89 nH	1.79 pF

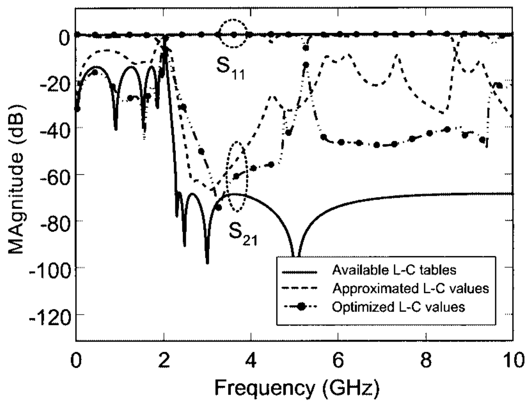

Fig. 8. Simulated frequency responses of the filter using four cascaded hairpin resonators.

C_{gt} is the capacitance chosen from the available *L-C* tables. In this case, the 3-dB cutoff frequency of the filter will be smaller than that of the filter using the available *L-C* tables. To obtain a proper 3-dB cutoff frequency, an alternative approximate method is used. In the beginning, one can use the capacitance and inductance C_1, L_2 in the available *L-C* tables and (3b), (6a), (7a), and (7b) to calculate C_2, C_{s1}, and C_{p1}, where the subscripts of $s1$ and $p1$ are the capacitances associated with the first resonator. Using C_3 and L_4 in the available *L-C* tables and (3b), (6a), (7a), and (7b), the capacitances C_4, C_{s2}, and C_{p2} can then be obtained. Thus, the total synthesized value for C_3 is given by

$$C_3(\text{syn.}) = C_{p1}+C_{s1}+2C_\Delta+C_{p2}+C_{s2}+C_{sp}\,l_c. \quad (10)$$

Furthermore, by adjusting the capacitance C_{sp} value (size of a adjacent microstrip line), one can obtain C_3 $(L\text{-}C \text{ tables}) = C_3$ (syn.). If the sum of the capacitances $C_{pl}+C_{sl}+2C_\Delta+C_{p2}+C_{s2}$ is larger than C_3 (*L-C* tables), the capacitance C_{sp} may be selected by a proper size of a microstrip line to link two resonators. The rest of the synthesized *L-C* values can be found by using the same procedure. Fig. 8 shows the simulated frequency responses of the filter using the available *L-C* tables, approximated *L-C* values, and optimized *L-C* values shown in Table II. Observing the simulated results of the filter using the approximated *L-C* values in Fig. 8, a 3-dB cutoff frequency close to 2 GHz is shown, but with harmonics at the stopband. These harmonics at the stopband are due to the different *L-C* values (sizes) of the hairpin resonators.

To reduce the harmonics at the stopband, an optimized filter constructed by identical hairpin resonators is used. Furthermore, during the optimization, it can be found that the filter can achieve a low return loss by using a long single transmission line and short coupled lines. The optimized *L-C* values are listed in Table II. Inspecting the simulated results in Fig. 8, the optimized filter using identical hairpin resonators can reduce harmonics at the stopband and provide a low return loss in the passband.

The optimized dimensions of the filter in Fig. 6(a) are $l_3 = 3.2$ mm, $l_4 = 12.02$ mm, $w_4 = w_6 = 0.8$ mm, and $w_5 = 2$ mm. l_f, w_1, w_2, w_3, and g are the same dimensions as before. The measured and simulated frequency responses of the optimized filter are shown in Fig. 9. This low-pass filter provides a much sharper cutoff frequency response and deeper rejection band compared to the results of using the one hairpin resonator given in Section III-A. This filter has a 3-dB passband from dc to 2.02 GHz. The return loss is better than 14 dB from dc to 1.96 GHz. The insertion loss is less than 0.6 dB. The rejection is greater than 42 dB from 2.68 to 4.93 GHz. The ripple is ±0.23 dB, as shown in Fig. 9(b).

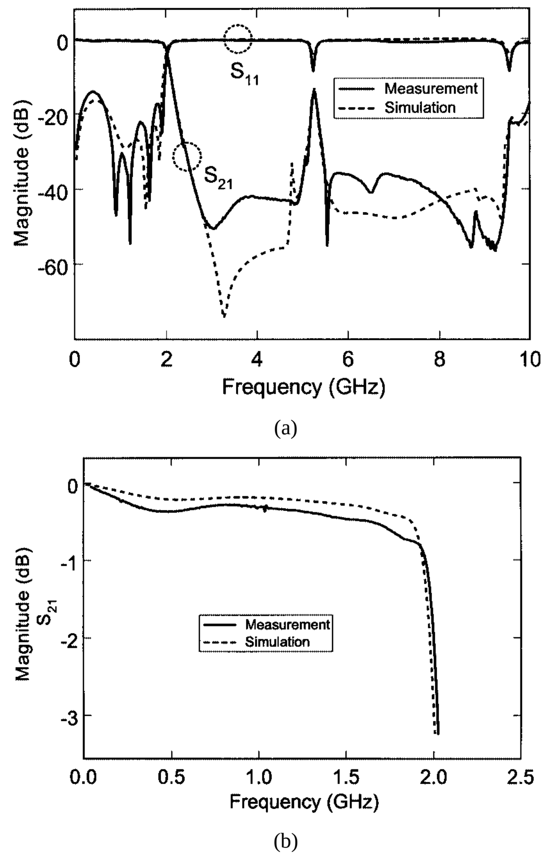

Fig. 9. Measured and simulated: (a) frequency response and (b) S_{21} within the 3-dB bandwidth for the filter using cascaded hairpin resonators.

C. Broad Stopband Low-Pass Filter

Observing the frequency response of the low-pass filter in Fig. 9, the stopband bandwidth is limited by harmonics, especially for the second harmonic. In order to extend the stopband bandwidth, additional attenuation poles at the second harmonic can be added. The additional attenuation poles can be implemented by additional low-pass filter using two cascaded hairpin resonators with a higher 3-dB cutoff frequency and attenuation at the second harmonic, as shown in Fig. 10. The desired higher 3-dB cutoff and attenuation frequencies of the additional low-pass filter can be obtained by using a similar synthesis procedure as discussed in Section III-A. The optimized dimensions of the additional low-pass filter are $l_5 = 2.55$ mm, $l_6 = 10.02$ mm, and $w_7 = 0.5$ mm. l_f, w_1, w_2, w_3, and g have the same dimensions as shown earlier in Section III-B. Fig. 11(a) shows the measured and simulated results. The additional low-pass filter attenuates the level of the second harmonic and achieve a wider stopband bandwidth with attenuation better than 33.3 dB from 2.45 to 10 GHz. The return loss of the filter is

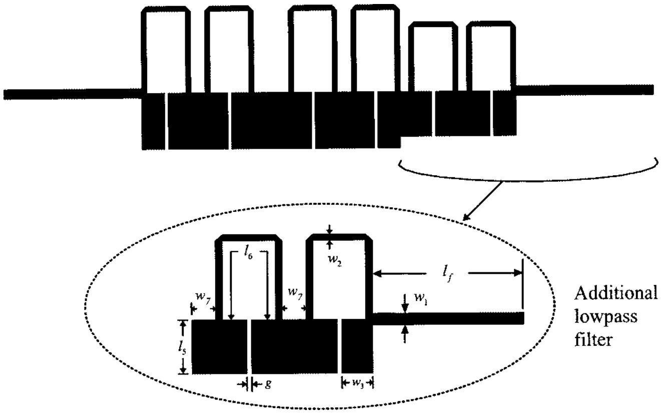

Fig. 10. Layout of the low-pass filter with additional attenuation poles.

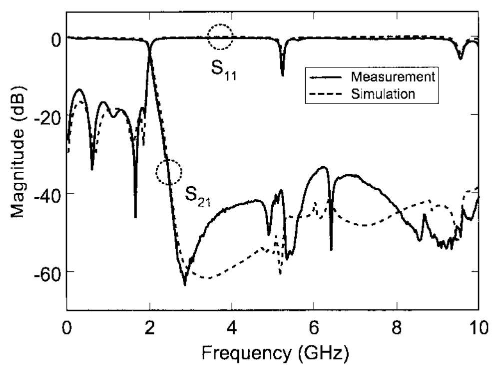

(a)

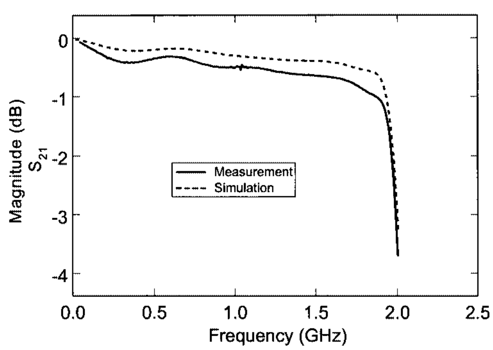

(b)

Fig. 11. Measured and simulated: (a) frequency response and (b) S_{21} within the 3-dB bandwidth for the filter with additional attenuation poles.

greater than 13.6 dB within dc to 1.94 GHz. The insertion loss is less than 1 dB. As seen in Fig. 11(b), the ripple is ±0.33 dB.

IV. Conclusions

Compact elliptic-function low-pass filters using stepped-impendance hairpin resonators have been proposed. The filters have been synthesized and optimized from the equivalent lumped-element model using the available element-value tables and EM simulation. The low-pass filter using multiple cascaded stepped-impendance hairpin resonators have shown a very sharp cutoff frequency response and low insertion loss. Moreover, with additional attenuation poles, the low-pass filter can obtain a wide stopband bandwidth. The measured results of the low-pass filters agree well with simulated results. The useful equivalent-circuit model for the stepped-impendance hairpin resonator provides a simple method to design filters and other circuits.

Acknowledgment

The authors would like to thank C. Wang, Texas A&M University, College Station, for his technical assistance and C. Rodenbeck, Texas A&M University, for his helpful discussions.

References

[1] J. S. Won, “Microstrip tapped-line filter design,” *IEEE Trans. Microwave Theory Tech.*, vol. MTT-27, pp. 44–50, Jan. 1979.

[2] M. Sagawa, K. Takahashi, and M. Makimot, “Miniaturized hairpin resonator filters and their application to receiver front-end MIC’s,” *IEEE Trans. Microwave Theory Tech.*, vol. 37, pp. 1991–1997, Dec. 1989.

[3] J. T. Ku, M. J. Maa, and P. H. Lu, “A microstrip elliptic function filter with compact miniaturized hairpin resonator,” *IEEE Microwave Guided Wave Lett.*, vol. 10, pp. 94–95, Mar. 2000.

[4] S. Y. Lee and C. M. Tsai, “New cross-coupled filter design using improved hairpin resonators,” *IEEE Trans. Microwave Theory Tech.*, vol. 48, pp. 2482–2490, Dec. 2000.

[5] J. T. Kuo, M. J. Maa, and P. H. Lu, “Microstrip elliptic function filters with compact miniaturized hairpin resonators,” in *Asia–Pacific Microwave Conf.*, 1999, pp. 860–864.

[6] A. Enokihara, K. Setsune, M. Sagawa, and M. Makimoto, “High-T_C bandpass filter using miniaturized microstrip hairpin resonator,” *Electron. Lett.*, vol. 28, no. 20, pp. 1925–1927, Sept. 1992.

[7] D. M. Pozar, *Microwave Engineering*. New York: Wiley, 1998, vol. 2nd, ch. 8.

[8] I. Rumsey, M. Piket-May, and P. K. Kelly, “Photonic bandgap structure used as filters in microstrip circuits,” *IEEE Microwave Guided Wave Lett.*, vol. 8, no. 10, pp. 336–338, Oct. 1998.

[9] D. Ahn, J. S. Park, C. S. Kim, J. Kim, Y. Qian, and T. Itoh, “A design of the low-pass filter using the novel microstrip defected ground structure,” *IEEE Trans. Microwave Theory Tech.*, vol. 49, pp. 86–92, Jan. 2001.

[10] J. W. Sheen, “A compact semilumped low-pass filter for harmonics and spurious suppression,” *IEEE Microwave Guided Wave Lett.*, vol. 10, pp. 92–93, Mar. 2000.

[11] L.-H. Hsieh and K. Chang, “Compact lowpass filter using stepped impedance hairpin resonator,” *Electron. Lett.*, vol. 37, no. 14, pp. 899–900, July 2001.

[12] F. Giannini, M. Salerno, and R. Sorrentino, “Design of low-pass elliptic filters by means of cascaded microstrip rectangular elements,” *IEEE Trans. Microwave Theory Tech.*, vol. 30, pp. 1348–1353, Sept. 1982.

[13] H. Yabuki, M. Sagawa, and M. Makimoto, “Voltage controlled push–push oscillators using miniaturized hairpin resonators,” in *IEEE MTT-S Int. Microwave Symp. Dig.*, 1991, pp. 1175–1178.

[14] C.Brian Wadell, *Transmission Line Design Handbook*. Norwood, MA: Artech House, 1991, p. 321.

[15] P. R. Geffe, *Simplified Modern Filter Design*. New York: John F. Rider, 1963, sec. Appendix 4.

[16] G. Mazzarella, “CAD modeling of interdigitated structures,” *IEEE Trans. Educ.*, vol. 42, pp. 81–87, Feb. 1999.

Lung-Hwa Hsieh (S’01) was born in Panchiao, Taiwan, R.O.C., in 1969. He received the B.S. degree in electrical engineering from Chung Yuan Christian University, Chungli, Taiwan, R.O.C., in 1991, the M.S. degree in electrical engineering from the National Taiwan University of Science and Technology, Taipei, Taiwan, R.O.C., in 1993, and is currently working toward the Ph.D. degree in electrical engineering at Texas A&M University, College Station.

From 1995 to 1998, he was a Senior Design Engineer with General Instrument, Taipei, Taiwan, R.O.C., where he was involved in RF video and audio circuit design. Since 2000, he has been a Research Assistant with the Department of Electrical Engineering, Texas A&M University. His research interests include microwave integrated circuits and devices.

Kai Chang (S'75–M'76–SM'85–F'91) received the B.S.E.E. degree from the National Taiwan University, Taipei, Taiwan, R.O.C., in 1970, the M.S. degree from the State University of New York at Stony Brook, in 1972, and the Ph.D. degree from The University of Michigan at Ann Arbor, in 1976.

From 1972 to 1976, he was with the Microwave Solid-State Circuits Group, Cooley Electronics Laboratory, The University of Michigan at Ann Arbor, where he was a Research Assistant. From 1976 to 1978, he was with Shared Applications Inc., Ann Arbor, MI, where he was involved with computer simulation of microwave circuits and microwave tubes. From 1978 to 1981, he was with the Electron Dynamics Division, Hughes Aircraft Company, Torrance, CA, where he was involved in the research and development of millimeter-wave solid-state devices and circuits, power combiners, oscillators, and transmitters. From 1981 to 1985, he was with TRW Electronics and Defense, Redondo Beach, CA, where he was a Section Head involved with the development of state-of-the-art millimeter-wave integrated circuits and subsystems, including mixers, voltage-controlled oscillators (VCOs), transmitters, amplifiers, modulators, upconverters, switches, multipliers, receivers, and transceivers. In August 1985, he joined the Electrical Engineering Department, Texas A&M University, College Station, as an Associate Professor, and became a Professor in 1988. In January 1990, he became an E-Systems Endowed Professor of Electrical Engineering. He has authored and coauthored several books, including *Microwave Solid-State Circuits and Applications* (New York: Wiley, 1994), *Microwave Ring Circuits and Antennas* (New York: Wiley, 1996), *Integrated Active Antennas and Spatial Power Combining* (New York: Wiley, 1996), and *RF and Microwave Wireless Systems* (New York: Wiley, 2000). He has served as the Editor of the four-volume *Handbook of Microwave and Optical Components* (New York: Wiley, 1989 and 1990). He is the Editor of *Microwave and Optical Technology Letters* and the Wiley Book Series on "Microwave and Optical Engineering." He has also authored or coauthored over 350 technical papers and several book chapters in the areas of microwave and millimeter-wave devices, circuits, and antennas. His current interests are microwave and millimeter-wave devices and circuits, microwave integrated circuits, integrated antennas, wide-band and active antennas, phased arrays, microwave power transmission, and microwave optical interactions.

Dr. Chang was the recipient of the 1984 Special Achievement Award presented by TRW, the 1988 Halliburton Professor Award, the 1989 Distinguished Teaching Award, the 1992 Distinguished Research Award, and the 1996 Texas Engineering Experiment Station (TEES) Fellow Award presented by Texas A&M University.